IEEE Access
Multidisciplinary : Rapid Review : Open Access Journal

Received December 1, 2018, accepted January 14, 2019, date of publication January 21, 2019, date of current version February 8, 2019.

Digital Object Identifier 10.1109/ACCESS.2019.2893910

Optimal Planning of Multi-Energy System Considering Thermal Storage Capacity of Heating Network and Heat Load

HONGZHONG CHENG[1], JIAN WU[1], ZHAO LUO[2], (Member, IEEE), FEI ZHOU[1], XINGLIN LIU[2], AND TAO LU[2]

[1]State Grid Suzhou Power Supply Company, Suzhou 215004, China
[2]Faculty of Electric Power Engineering, Kunming University of Science and Technology, Kunming 650500, China

Corresponding author: Zhao Luo (waiting.1986@live.com)

This work was supported in part by the National Natural Science Foundation of China under Grant 51607036, in part by the ADN Comprehensive Demonstration Project of Smart Grid Application Demonstration Area in Suzhou Industrial Park, in part by the Yunnan Provincial Talents Training Program under Grant KKSY201704027, and in part by the Scientific Research Foundation of the Yunnan Provincial Department of Education under Grant 2018JS032.

ABSTRACT The multi-energy system (MES) is believed to have bright prospects in the future for its advantages of high energy efficiency, flexible operation condition, and environmentally friendly. The heating network and the heat load play an important role in the MES and have great potentials in improving the system performance. In this paper, an optimal planning method is proposed for the MES that considers the thermal storage capacity of the heating network and the heat load. The objective includes the investment cost, the fuel cost, the grid cost, the maintenance cost, and the environmental cost. The constraints of the cogeneration, the heating network, and the heat load are all taken into consideration. The simulation based on the typical working conditions in annual operation is performed to verify the effectiveness of the proposed planning method. Four cases are set in order to comprehensively investigate the effect of the thermal storage capacity of the heating network and the heat load on the MES planning. The results indicate that the proposed method can decrease the capacity of the devices and reduce the fuel cost.

INDEX TERMS Heat load, heating network, multi-energy system (MES), optimal planning, thermal storage capacity.

I. INTRODUCTION

Energy is an important foundation for the development of human society and constructing an efficient, clean, and sustainable energy system is a crucial problem faced by human being at present. Compared with traditional separated energy system, the multi-energy system (MES) is a kind of energy system that integrates multi kinds of energy carrier and provides energy service for different kinds of demand, which has many advantages including high energy efficiency, flexible operation condition, environmentally friendly and so on [1]–[3]. Therefore, the MES is believed to have bright prospects in the future [3]–[5]. At the distribution level or the microgrid level, the most common form of the MES is the integrated heat and power microgrid, which consists of the cogeneration system, the heating system, and loads. For the integrated heat and power MES, the most basic and core issue to improve the energy efficiency and the economic performance is to realize the coordinated planning of electricity and heat [6]–[10].

At present, many researches on the planning of the MES have been conducted and the focus include the system structure optimization, the capacity configuration of the units, and the configuration of the energy storage system and so on. In [10], both the structure configuration and the capacity configuration are combined in a generic planning framework of the smart MES and a mixed-integer linear programming (MILP) based planning model was proposed to minimize the cost of the smart MES. In [11], a novel optimization model of the hybrid energy storage system was proposed for the combined heat and power (CHP) system, where the state of charge, the current, and the capacity of the hybrid energy storage system were comprehensively taken into consideration in the optimization model. In [12], an novel optimal design model was proposed for a MES that involves seasonal energy storage and the proposed methodology allows taking to consideration a year time horizon with hour resolution so that the complexity of the problem can be greatly reduced. In [13], a bilevel model construction method is proposed for the configuration of the combined cooling, heating, and power (CCHP) coupled MES and a CCHP coupling MES optimization toolbox based on the sequential quadratic programming and feedback correction method was developed in a Matlab environment.

However, the concentrations of the above researches are limited to the planning cogeneration system. As important parts of the MES, the heating network and the heat load play important role in coordinating the heat and power production and thus have great potentials in improving the performance of the MES [14]–[19]. The heating network links the cogeneration system with the heat load and its physical characteristics including the transmission delay, heat loss, and thermal storage capacity have important influence on the operation of the MES. In [20], a simplified model was established for heating network that ignored the transmission delay and based on that the effect of the heating network on the operational cost of the MES was researched. The results showed that the operational cost of MES can be reduced by the utilization of the heating network. In [21], a multi-objective optimization model considering the energy and economic performance was proposed for the design of the CHP-heating network system. On another hand, the flexibility of the heat load brings itself thermal storage capacity and provide considerable flexible space for the heating supply so as to provide ignorable improvement potential for the planning and operation of the MES [22]–[25]. In [26], an integrated demand response (IDR) concept was proposed that combines the electrical load response and the heating/cooling load response, and the simulation results indicated that the IDR programming can improve the economic performance of the energy hub. In [27], a daily dispatching model was proposed for a building MES where the room temperature control is applied to determine the flexible heat demand. In summary, the characteristics of the heat load have been researched for the MES mainly from the viewpoint of operation.

Above all, the thermal storage capacity of the heating network and the heat load has great potentials in improving the economic and environmental performance of the MES. Although the coordinated dispatch of the MES with heating network and flexible heat load has also gained some researches, the benefits of the heating network and the heat load in the MES planning have not been investigated adequately and the related studies are few. Therefore, we investigate the planning problem of the MES considering the thermal storage capacity of the heating network and the heat load. The characteristics of the heating network are modeled accurately and comprehensively based on the node method. The heat load including the building heating load and domestic hot water load is modeled based on the thermal model of buildings and water storage tank. Based on this, an optimal planning model based on MILP is proposed for the MES and the investment cost, the fuel cost, the grid cost, the maintenance cost, and the environmental cost are all considered in the objective. The results of the case studied show that when considering the thermal storage capacity of the heating network and the heat load, (1) the necessary capacity of the gas boiler, the battery, and the thermal storage can be decreased; (2) the fuel cost is reduced; and (3) the utilization ratio of the gas turbine is high in both winter and transition seasons.

The rest of the paper is organized as follows. In Section II, the optimal planning model of the MES is comprehensively formulated. In Section III, the simulations are performed and the results are analyzed. Conclusions are presented in Section IV.

II. OPTIMAL PLANNING MODEL OF THE MES

A. OBJECTIVE

The objective of the optimal planning model of the MES is given in (1), which include both the economic cost and the environmental cost. The economic cost includes the annualized investment cost C_{inv}, the fuel cost C_{fuel}, the interacting cost with the main grid C_{grid}, and the maintenance cost C_{main}. The environmental cost C_{env} includes the penalty cost for the carbon dioxide produced by the gas turbine and the gas boiler.

$$\min C = C_{inv} + C_{fuel} + C_{grid} + C_{main} + C_{env} \tag{1}$$

The annualized investment cost takes into consideration the gas turbine, the gas boiler, the battery, and the thermal storage tank as follows, where r is the capital interest rate, y is investment return years, C_{gt}^{inv} and C_{gb}^{inv} are the unit capacity investment cost of the gas turbine and the gas boiler, respectively, C_{bt}^{inv} and C_{tst}^{cap} are the unit capacity investment cost of the battery and the thermal storage tank, respectively, P_{gt}^{cap} and Q_{gb}^{cap} are the capacity of the gas turbine and the gas boiler, respectively, and E_{gt}^{cap} and E_{tst}^{cap} are the capacity of the battery and the thermal storage tank, respectively.

$$C_{inv} = \frac{r(1+r)^y}{(1+r)^y - 1} \begin{pmatrix} c_{gt}^{inv} P_{gt}^{cap} + c_{gb}^{inv} Q_{gb}^{cap} \\ + c_{bt}^{inv} E_{bt}^{cap} + c_{tst}^{inv} E_{tst}^{cap} \end{pmatrix} \tag{2}$$

The fuel cost includes the natural gas cost of the gas turbine and the gas boiler as follows, where c_{gas} is the price of the natural gas, P_{gt}^t is the electrical power of the gas turbine at time period t, Q_{gb}^t is the heat power of the gas boiler at time period t, η_{gt} is the efficiency of the gas turbine, η_{gb} is the efficiency of the gas boiler, t is the time interval of the period, and N is the index set of time period.

$$C_{fuel} = c_{gas} \sum_{t \in \mathrm{N}} \frac{P_{gt}^t}{\eta_{gt}} \Delta t + c_{gas} \sum_{t \in \mathrm{N}} \frac{Q_{gb}^t}{\eta_{gb}} \Delta t \tag{3}$$

The interacting cost with the main grid is equal to the cost of purchasing electricity from the main grid minus the revenue of selling electricity to the main grid as follows, where $C_{grid}^{b,t}$ is the price of electricity purchased from the main grid, $C_{grid}^{s,t}$ is the price of electricity sold to the main grid, and

$P_{grid}^{b,t}$ and $P_{grid}^{s,t}$ are the electrical power of purchasing from and sold to the main grid at time period t, respectively

$$C_{grid} = \sum_{t \in N} c_{grid}^{b,t} P_{grid}^{b,t} \Delta t - \sum_{t \in N} c_{grid}^{s,t} P_{grid}^{s,t} \Delta t \tag{4}$$

The maintenance cost takes into consideration the gas turbine, the gas boiler, the battery, and the thermal storage tank as follows, where C_{gt}^{om} and C_{gb}^{om} are unit maintenance cost of the gas turbine and the gas boiler, respectively, C_{bt}^{om} and C_{tst}^{om} are unit maintenance cost of the battery and the thermal storage tank, respectively, $P_{bt}^{chr,t}$ and $P_{bt}^{dis,t}$ are charging power and discharging power of the battery, respectively, and $Q_{bt}^{chr,t}$ and $Q_{bt}^{dis,t}$ are storing power and releasing power of the thermal storage tank, respectively.

$$C_{main} = \sum_{t \in N} \begin{pmatrix} c_{gt}^{om} P_{gt}^{t} + c_{gb}^{om} Q_{gb}^{t} + c_{bt}^{om} P_{bt}^{chr,t} \\ + c_{bt}^{om} P_{bt}^{dis,t} + c_{tst}^{om} Q_{tst}^{chr,t} + c_{tst}^{om} Q_{tst}^{dis,t} \end{pmatrix} \tag{5}$$

The environmental cost of the MES is as follows, where c_{pena} is unit penalty cost for CO_2 emission, m_{gt} is the CO_2 emission factor of the gas turbine, and m_{gb} is the CO_2 emission factor of the gas boiler.

$$C_{env} = c_{pena} \sum_{t \in N} \left(m_{gt} P_{gt}^{t} + m_{gb} Q_{gb}^{t} \right) \tag{6}$$

B. CONSTRAINTS

1) COGENERATION SYSTEM

In the cogeneration system, the devices such the gas turbine, the gas boiler, the battery, and the thermal storage tank have their own operational constraints. The operational constraints of the gas turbine and the gas boiler are as follows, where Q_{gt}^{t} is the output thermal power of the gas turbine and α is the power to heat ratio. The first constraint is the limitation of output electrical power of the gas turbine, the second constraint is the equation of power to heat equation, and the third constraint is the limitation of output heat power of the gas boiler.

$$0 \le P_{gt}^{t} \le P_{gt}^{cap}, \quad Q_{gt}^{t} = \alpha P_{gt}^{t}, \; 0 \le Q_{gb}^{t} \le Q_{gb}^{cap} \tag{7}$$

The operational constraints of the battery are given as

$$\begin{cases} 0 \le P_{bt}^{chr,t} \le \varepsilon_{bt}^{chr,t} \lambda_{bt}^{chr} E_{bt}^{cap} \\ 0 \le P_{bt}^{dis,t} \le \varepsilon_{bt}^{dis,t} \lambda_{bt}^{dis} E_{bt}^{cap} \\ \varepsilon_{bt}^{chr,t} + \varepsilon_{bt}^{dis,t} = 1, \quad \varepsilon_{bt}^{chr,t}, \; \varepsilon_{bt}^{dis,t} \in \{0,1\} \\ E_{bt}^{t+1} = E_{bt}^{t} + \left(\eta_{bt}^{chr} P_{bt}^{chr,t} - P_{bt}^{dis,t} \big/ \eta_{bt}^{dis} \right) \Delta t \\ \pi_{bt}^{low} E_{bt}^{cap} \le E_{bt}^{t} \le \pi_{bt}^{up} E_{bt}^{cap} \end{cases} \tag{8}$$

where $\varepsilon_{bt}^{chr,t}$ and $\varepsilon_{bt}^{dis,t}$ are binary variables representing the state of charging and discharging, respectively, λ_{bt}^{chr} and λ_{bt}^{dis} are upper limit coefficient of charging and discharging, respectively, E_{bt}^{t} is the energy level of the battery, η_{bt}^{chr} and η_{bt}^{dis} are efficiency of charging and discharging, respectively, and π_{bt}^{low} and π_{bt}^{up} are lower limit coefficient and upper limit coefficient of the energy level, respectively. The first and the second constraints are limit of charging power and discharging power. The third and the fourth constraints are limitations of charging state and discharging state. The fifth constraint is the energy equation of the battery, and the last constraint is the limitations of energy level.

The operational constraints of the thermal storage tank are given in (9), where $\varepsilon_{tst}^{chr,t}$ and $\varepsilon_{tst}^{dis,t}$ are binary variables representing the state of storing and releasing, respectively, λ_{tst}^{chr} and λ_{tst}^{dis} are upper limit coefficient of storing and releasing, respectively, E_{tst}^{t} is the energy level of the thermal storage tank, η_{tst}^{chr} and η_{tst}^{dis} are efficiency of storing and releasing, respectively, and π_{tst}^{low} and π_{tst}^{up} are lower limit coefficient and upper limit coefficient of the energy level, respectively. The meaning of each constraints is similar with that of the battery.

$$\begin{cases} 0 \le Q_{tst}^{chr,t} \le \varepsilon_{tst}^{chr,t} \lambda_{tst}^{chr} E_{tst}^{cap} \\ 0 \le Q_{tst}^{dis,t} \le \varepsilon_{tst}^{dis,t} \lambda_{tst}^{dis} E_{tst}^{cap} \\ \varepsilon_{tst}^{chr,t} + \varepsilon_{tst}^{dis,t} = 1, \quad \varepsilon_{tst}^{chr,t}, \; \varepsilon_{tst}^{dis,t} \in \{0,1\} \\ E_{tst}^{t+1} = E_{tst}^{t} + \left(\eta_{tst}^{chr} Q_{tst}^{chr,t} - Q_{tst}^{dis,t} \big/ \eta_{tst}^{dis} \right) \Delta t \\ \pi_{tst}^{low} E_{tst}^{cap} \le E_{tst}^{t} \le \pi_{tst}^{up} E_{tst}^{cap} \end{cases} \tag{9}$$

Other constraints of the cogeneration system include the constraints of interacting with the main grid, the load transfer constraints, and the energy balance constraints. The constraints of interacting with the main grid are given in (10), where P_{grid}^{max} is the maximum interacting power, and $\varepsilon_{grid}^{b,t}$ and $\varepsilon_{grid}^{s,t}$ are binary variables representing the state of purchasing electricity from and selling electricity to the main grid. The first and the second constraints are limitations of interacting power. The third and the fourth constraints are limitations of the interacting state.

$$\begin{cases} 0 \le P_{grid}^{b,t} \le \varepsilon_{grid}^{b,t} P_{grid}^{\max} \\ 0 \le P_{grid}^{s,t} \le \varepsilon_{grid}^{s,t} P_{grid}^{\max} \\ \varepsilon_{grid}^{b,t} + \varepsilon_{grid}^{s,t} = 1, \quad \varepsilon_{grid}^{b,t}, \; \varepsilon_{grid}^{s,t} \in \{0,1\} \end{cases} \tag{10}$$

The constraints of load transfer are given in (11), where $\varepsilon_{load}^{in,t}$ and $\varepsilon_{load}^{out,t}$ are binary variables representing the state of transferring in and transferring out at time period t, respectively, and $P_{load}^{tra,t}$ is the transferable electrical load at time period t. The first and the second constraints are limitations of the electrical power transferred in and transferred out, respectively. The third and the fourth constraints are limitations of the transferring in and transferring out state.

$$\begin{cases} 0 \le P_{load}^{in,t} \le \varepsilon_{load}^{in,t} P_{load}^{tra,t} \\ 0 \le P_{load}^{out,t} \le \varepsilon_{load}^{out,t} P_{load}^{tra,t} \\ \varepsilon_{load}^{in,t} + \varepsilon_{load}^{out,t} = 1, \quad \varepsilon_{load}^{in,t}, \; \varepsilon_{load}^{in,t} \in \{0,1\} \end{cases} \tag{11}$$

The energy balance constraints are given in (12), where $P_{load}^{fix,t}$ is the fixed electrical load at time period t, $Q_{co}^{out,t}$ is the output heat power of the cogeneration system at time period t, and η_{he} is the efficiency of the heat exchanger. The first and the second constraints represent the electrical power balance and the thermal power balance, respectively.

$$\begin{cases} P_{gt}^{t} - P_{bt}^{chr,t} + P_{bt}^{dis,t} + P_{grid}^{b,t} - P_{grid}^{s,t} \\ \quad = P_{load}^{fix,t} + P_{load}^{in,t} - P_{load}^{out,t} \\ Q_{gt}^{t} + Q_{gb}^{t} - Q_{tst}^{chr,t} + Q_{tst}^{dis,t} = Q_{co}^{out,t} / \eta_{he} \end{cases} \tag{12}$$

2) HEATING NETWORK

A simple structure of the heating network is given in (12). The heating network consists of supply pipelines, return pipelines, and nodes. The structure of the supply network and the return network are mirrored and the same and hence, the return pipelines are neglected in FIGURE 1 The modeling of the heating network is based on the node method under quality-regulation operation mode The constraints of the heating network include the temperature mixing and energy conservation, the transmission delay and heat loss, and the temperature limit.

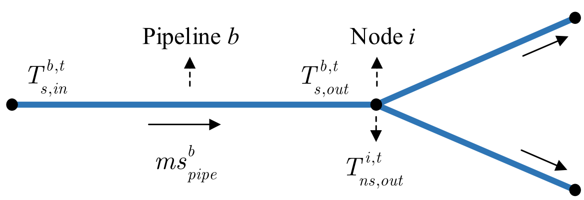

FIGURE 1. Simple structure of the heating network.

a: TEMPERATURE MIXING AND ENERGY CONSERVATION

Assuming that the mass flowing into the same node exchanges the heat energy and mixes their temperature fully, the mass that flows out of this node will have the same temperature, as given in (13). The first constraint is the temperature mixing at the nodes of supply pipelines while the second constraint is the temperature mixing at the nodes of return pipelines. Herein $T_{s,in}^{b,t}$ is the temperature of the mass flowing out from the supply pipeline b at time period t, $T_{r,in}^{b,t}$ is the temperature of the mass flowing out from the return pipeline b at time period t, $T_{ns}^{i,t}$ and $T_{nr}^{i,t}$ are temperature of mass at supply node i and return node i, respectively, I_{nd} is the indices set of node, Φ_{+}^{i} is the indices set of the pipelines which the mass from the node i flows into, and Φ_{-}^{i} is the indices set of the pipelines from which the mass flows into the node i

$$\begin{cases} T_{s,in}^{b,t} = T_{ns}^{i,t} & \forall i \in \mathrm{I}_{nd},\ b \in \Phi_{+}^{i},\ t \in \mathrm{N} \\ T_{r,in}^{b,t} = T_{nr}^{i,t} & \forall i \in \mathrm{I}_{nd},\ b \in \Phi_{-}^{i},\ t \in \mathrm{N} \end{cases} \tag{13}$$

According to the law of energy conservation, the thermal energy flowing into a node should be equal to that flowing out from this node and thus we can get the energy conservation constraints as given as

$$\begin{cases} \sum_{b \in \Phi_{pipe-}^{i}} \left(T_{s,out}^{b,t} \cdot ms_{pipe}^{b} \right) = T_{ns}^{i,t} \sum_{b \in \Phi_{pipe-}^{i}} ms_{pipe}^{b} \\ \forall i \in \mathrm{I}_{nd}, \quad t \in \mathrm{N} \\ \sum_{b \in \Phi_{pipe+}^{i}} \left(T_{r,out}^{b,t} \cdot ms_{pipe}^{b} \right) = T_{nr}^{i,t} \sum_{b \in \Phi_{pipe+}^{i}} ms_{pipe}^{b} \\ \forall i \in \mathrm{I}_{nd}, \quad t \in \mathrm{N} \end{cases} \tag{14}$$

where ms_{pipe}^{b} is the mass flow at the pipeline b. The first constraint and the second constraint indicate the energy conservation at the node of supply pipelines and at the node of return pipelines, respectively.

In addition, in the source node and the load node, the following constraints should be meet according to energy conservation. The first constraint indicates the energy balance at the source node, where c is the specific heat capacity of the mass and Φ_{src} is the indices set of the pipelines connecting to the source node. The Second constraint is the energy balance at the heat load node, where $Q_{hn}^{i,t}$ is the heat demand at the node i at time period t, Φ_{hl}^{i} is the indices set of the pipelines connecting to the node i, and I_{nd}^{hl} is the indices set of the heat load node.

$$\begin{cases} Q_{co}^{out,t} = c \cdot \sum_{b \in \Phi_{src}} ms_{pipe}^{b} \left(T_{s,in}^{b,t} - T_{r,out}^{b,t} \right) \\ Q_{hn}^{i,t} = c \cdot ms_{pipe}^{b} \left(T_{s,out}^{b,t} - T_{r,in}^{b,t} \right) \\ \quad b \in \Phi_{hl}^{i}, \quad \forall i \in \mathrm{I}_{nd}^{hl} \end{cases} \tag{15}$$

b: TRANSMISSION DELAY AND HEAT LOSS

The modeling of the transmission delay and loss is based on the node method. Firstly, the temperature of the mass flow is calculated by (16) where the heat loss is ignored temporarily. Herein, $T_{s,out}^{\prime b,t}$ and $T_{r,out}^{\prime b,t}$ are the estimated temperature of mass flowing out of the supply pipeline b and the return pipeline b at time period t, respectively, $T_{s,in}^{b,t}$ and $T_{r,in}^{b,t}$ are the temperature of mass flowing into the supply pipeline b and the return pipeline b at time period t, respectively, β^{b} and γ^{b} are integer constants to denote the time delays of the mass flow in pipeline b, $K^{b,k}$ is the coefficient, and Φ is the indices set of pipelines.

$$\begin{cases} T_{s,out}^{\prime b,t} = \sum_{k=t-\beta^{b}}^{t-\gamma^{b}} K^{b,k} T_{s,in}^{b,k} & \forall b \in \Phi,\ t \in \mathrm{N} \\ T_{r,out}^{\prime b,t} = \sum_{k=t-\beta^{b}}^{t-\gamma^{b}} K^{b,k} T_{r,in}^{b,k} & \forall b \in \Phi,\ t \in \mathrm{N} \end{cases} \tag{16}$$

The constants γ^{b}, β^{b}, and $K^{b,k}$ can be calculated as (17)-(18). In(17), Z is the integer set, ρ is the density of the mass flow, A^{b} is the cross-sectional area of pipeline b, and I^{b} is the length of pipeline b. In (18), R^{b} is the total mass that flows into the pipeline b from time period $t - \gamma^{b}$ to t and it can be calculated by (19).

$$\gamma^b = \min_n \left\{ \begin{array}{l} n : s.t.\ (n+1)\cdot\left(ms^b_{pipe}\Delta t\right) \\ \geq \rho A^b l^b, n \geq 0, n \in Z \end{array} \right\}$$
$$\beta^b = \min_m \left\{ \begin{array}{l} m : s.t.\ m\cdot\left(ms^b_{pipe}\Delta t\right) \\ \geq \rho A^b l^b, m \geq 0, m \in Z \end{array} \right\} \tag{17}$$

$$K^{b,k} = \begin{cases} \left(\rho A^b l^b + ms^b_{pipe}\Delta t - R^b\right) \Big/ \left(ms^b_{pipe}\Delta t\right), \\ \quad k = t - \beta^b \\ 1, \quad k = t - \beta^b + 1, \cdots, t - \gamma^b - 1 \\ \left(R^b - \rho A^b l^b\right) \Big/ \left(ms^b_{pipe}\Delta t\right), \\ \quad k = t - \gamma^b \\ 0 \quad otherwise \end{cases} \tag{18}$$

$$R^b = (\gamma^b + 1)\left(ms^b_{pipe}\Delta t\right) \tag{19}$$

Secondly, the heat loss should be taken into consideration which is reflected by the temperature drop. The actual temperature of mass flowing out of the pipeline b can be calculated by (20), where $T^{b,t}_{s,out}$ and $T^{b,t}_{r,out}$ are the actual temperature of mass flowing out of the supply pipeline b and the return pipeline b at time period t, respectively, T^t_{am} is the ambient temperature of the heating network, ξ^b is the temperature drop ratio, and λ^b is the heat transfer coefficient of pipeline b

$$\begin{cases} T^{b,t}_{s,out} = T^t_{am} + \left(T'^{b,t}_{s,out} - T^t_{am}\right)\cdot \xi^b \\ T^{b,t}_{r,out} = T^t_{am} + \left(T'^{b,t}_{r,out} - T^t_{am}\right)\cdot \xi^b \\ \xi^b = \exp\left[-\frac{\lambda^b \Delta t}{A^b \rho c}\left(\gamma^b + \frac{3}{2} + \frac{\rho A^b l^b - R^b}{ms^b_{pipe}\Delta t}\right)\right] \end{cases} \tag{20}$$

3) TEMPERATURE LIMIT

In addition the following constraints should be included in order to ensure the quality of the heating supply. Herein, T^{min}_s and T^{max}_s are the minimum and the maximum value of temperature in the supply pipeline, respectively, and T^{min}_r and T^{max}_r are the minimum and the maximum value of temperature in the return pipeline, respectively,

$$\begin{cases} T^{\min}_s \leq T^{b,t}_{s,in}, \quad T^{b,t}_{s,out} \leq T^{\max}_s \\ T^{\min}_r \leq T^{b,t}_{r,in}, \quad T^{b,t}_{r,out} \leq T^{\max}_r \end{cases} \tag{21}$$

4) HEAT LOAD

The heat load of end users includes the building heating load and the domestic hot water load. The building heating load is to keep the indoor temperature at a comfort range. The indoor temperature equation of the building is given in (22) based on the thermal model of buildings, where $T^{i,t}_{in}$ is the indoor temperature at the heat load node i at time period t, R^i is the thermal resistance of the building at heat load node i, C^i_{air} is the heat capacity of indoor air at the load node i, B^i is number of buildings at the heat load node i, $Q^{i,t}_{hl,1}$ is the heat power supplied to the load node i for building heating at time period t, and T^t_{out} is the outdoor temperature at time period t

In order to keep the quality of the heating supply at a good level, the indoor temperature should be within a range and the average value during the dispatch period should be equal to the optimal value as given in (23). Herein, T^{min}_{in} and T^{max}_{in} are the minimum the maximum comfort indoor temperature, respectively, T^{opt}_{in} is the optimal indoor temperature, and N_d is the numbers of the time period in a day

$$T^{i,t+1}_{in} = T^{i,t}_{in}\cdot\exp\left(-\frac{\Delta t}{R^i C^i_{air}}\right) + \left(\frac{R^i Q^{i,t}_{hl,1}}{B^i} + T^t_{out}\right) \times \left(1 - \exp\left(-\frac{\Delta t}{R^i C^i_{air}}\right)\right) \quad \forall i \in I^{hl}_{nd} \tag{22}$$

$$T^{\min}_{in} \leq T^{i,t}_{in} \leq T^{\max}_{in}, \quad \sum_{t\in N} T^{i,t}_{in} = N_d \cdot T^{opt}_{in} \tag{23}$$

We assume that each user has installed a water storage tank at home to maintain a good hot water supply. The water storage tank absorbs the heat power from the heating network and the water temperature can be calculated by (24). Herein, $T^{i,t}_w$ is the temperature of the hot water at load node i at time period t, $V^{i,t}_{w,out}$ is the hot water volume consumed by users at load node i at time period t, V^i_w is the total volume of the water storage tank of users at load node i, T^{cold}_w is the temperature of cold water supplemented into the water storage tank, and $Q^{i,t}_{hl,2}$ is the heat power supplied to the load node i for domestic hot water at time period t. To ensure the user comfort, the temperature limit should be included as given in (25), where T^{min}_w and T^{max}_w are the minimum and the maximum comfort water temperature, respectively, and T^{opt}_w is the optimal water temperature. In addition, the heat power balance equation should be also include d as given in (26).

$$T^{i,t+1}_w = T^{i,t}_w - V^{i,t}_{w,out}\Big/V^i_w \cdot \left(T^{i,t}_w - T^{cold}_w\right) + Q^{i,t}_{hl,2}\Big/\left(c\cdot B^i\cdot V^i_w\right) \tag{24}$$

$$T^{\min}_w \leq T^{i,t}_w \leq T^{\max}_w, \quad \sum_{t\in N} T^{i,t}_w = N_d\cdot T^{opt}_w \tag{25}$$

$$Q^{i,t}_{hl} = Q^{i,t}_{hl,1} + Q^{i,t}_{hl,2} \tag{26}$$

C. MODEL SOLUTION

In summary, we have formulated a comprehensive optimal planning model (OPM) for the MES that takes into consideration the characteristics of the cogeneration system, the heating network, and the heat load. The thermal inertia of the heat load is utilized in the planning model to improve the flexibility of the MES. The OPM is a mixed integer linear programming (MILP) and I can be easily solved by on-the-shelf solvers such as CPLEX, Gurobi, and so on.

III. CASE STUDIES

In order to verify the economic performance of the proposed planning method, four cases under the background of North China are studied for comparison. The case I is a traditional planning method where the characteristics of both the heating network and the heat load is ignored; the case II only takes

TABLE 1. Optimal capacity of devices in different cases.

Case	Heating network	Heat load	Gas turbine (MW)	Gas boiler (MW)	Battery (kWh)	Thermal storage tank (kWh)
I	×	×	4.58	3.40	622	730
II	×	√	4.46	2.67	1009	520
III	√	×	4.61	2.67	30	120
IV	√	√	4.58	2.22	0	0

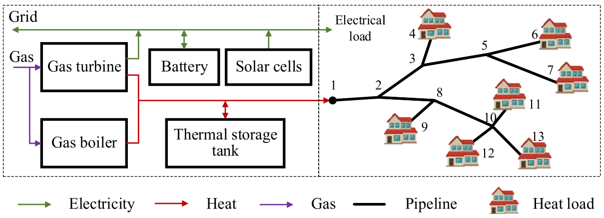

FIGURE 2. Structure of the cogeneration system and the heating network.

the characteristics of the heat load into consideration; the case III only takes the thermal storage capacity of the heating network into consideration; and the case IV utilizes both the characteristics of the heating network and the heat load. The simulation is performed on a laptop with Intel i7 CPU and 8GB RAM. The programming is in the environment of Matlab 2016a and the CPLEX is used to solve the model.

A. SYSTEM STRUCTURE AND PARAMETERS

The structure of the case is shown in FIGURE 2. The cogeneration system consists of a gas turbine, a gas boiler, solar cells, a battery, and a thermal storage tank. The cogeneration system can buy electricity from the main grid or sell electricity to it. We assume that the capacity of the solar cells are fixed and we need to optimize the capacity of the gas turbine, the gas boiler, the battery, and the thermal storage tank. The heating network consists of 12 supply pipelines and 7 nodes of heat load. The parameters of the devices in the cogeneration system is shown in Table 1. The parameters of the heating network and the heat load are given in Table 2 and Table 3, respectively.

TABLE 2. Parameters of devices in the cogeneration system.

Parameters	Value	Parameters	Value
r	6.5%	η_{he}	0.9
η_b	0.73	α	2.3
c_{gas}	0.3¥/kW	λ_{bt}^{chr}, λ_{bt}^{dis}	0.2,0.2
c_{gt}^{om}, c_{gb}^{om}	0.1,0.02¥/kW	η_{bt}^{chr}, η_{bt}^{dis}	0.95,0.95
c_{bt}^{om}, c_{tst}^{om}	0.05,0.01¥/kW	π_{bt}^{low}, π_{bt}^{up}	0.1,0.9
c_{comp}	0.1¥/kW	η_{tst}^{chr}, η_{tst}^{dis}	0.2,0.2
c_{pena}	0.15¥/kW	λ_{tst}^{chr}, λ_{tst}^{dis}	0.95,0.95
η_{gt}	0.3	π_{tst}^{low}, π_{tst}^{up}	0.1
η_{gb}	0.9	—	—

TABLE 3. Parameters of heating network.

Head	Tail	l (m)	Diameter (m)	λ (kW/(m·℃))	ms (t/h)
1	2	2000	0.40	0.25	230
2	3	1000	0.25	0.25	100
3	4	800	0.15	0.25	40
3	5	1000	0.25	0.25	60
5	6	800	0.15	0.25	30
5	7	1000	0.15	0.25	30
2	8	1000	0.25	0.25	130
8	9	500	0.15	0.25	30
8	10	1500	0.25	0.25	100
10	11	500	0.15	0.25	30
10	12	800	0.15	0.25	30
10	13	1000	0.15	0.25	40

There are three typical working condition in annual operation of the MES, i.e. winter, summer, and transition seasons. In the winter, the MES supplies thermal power to end users for the building heating and the domestic hot water. In the summer and transition seasons, the MES supplies thermal power only for domestic hot waters. In this case we assume that the durations of each work condition are 150, 80, and 135 days, respectively.

B. PLANNING RESULTS AND COST ANALYSIS

1) RESULTS OF OPTIMAL CAPACITY

The optimal capacity of each devices in the four cases are shown in Table 4. Firstly, the capacities of the gas turbine in

TABLE 4. Data of heat load.

NO	Node	C_{air} (kWh/℃)	R (℃/kW)	V_w (m^3)	B
1	4	0.5	6	50	200
2	6	0.5	6	50	150
3	7	0.5	6	50	150
4	9	0.6	7	60	150
5	11	0.6	7	60	150
6	12	0.6	7	60	150
7	13	0.6	7	60	200

different cases are very similar while those of the gas boiler are very different. The capacity of the gas boiler in the case IV is reduced by 34.7% compared with the case I and reduces by 17.6% compared with the case II and the case III. It can be concluded that the characteristics of the heating network and the heat load can effectively decrease the necessary capacity of the gas boiler. Secondly, the capacities of the battery in different cases have obvious differences. An interesting thing is that when only the thermal storage capacity of the heat load is considered (i.e. Case II), the capacity of the battery is increased compared with the case I. Thirdly, the capacities of the thermal storage tank show a downward trend from the case I to the case IV. In summary, we can see that taking the thermal storage capacity of the heating network and the heat load into consideration in the planning of the MES can reduce capacity of the gas boiler, the battery, and the thermal storage tank distinctly

2) COST ANALYSIS

The detailed cost in different cases are shown in Table 5 and Figure 3. The total cost shows a decreasing trend from the case I to IV. The total cost of the case IV is reduced by 9.4% compared with the case I. The total cost of the case II is very near to the case I and the cost of the case III is reduced by 3.7% compared with the case I. Therefore, we can conclude that the thermal storage capacity of the heating network brings more benefit to the planning of the MES compared with the heat load and simultaneously, we can obtain the most benefit to utilize the characteristics of both the heating network and the heat load at the same time in the MES planning. Moreover, it can be seen that the investment cost in each cases has little difference. For the case I, II, and IV, the fuel cost, the maintenance cost, and the environmental cost all show a decreasing trend while the grid cost shows an increasing trend. The case II is a special case and its total cost is nearly the same with the case I, which indicates that in this case only considering the characteristics of the heat load in the planning brings little benefits.

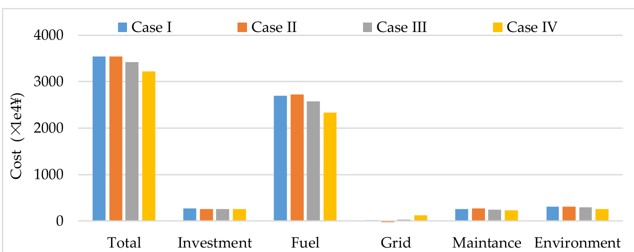

FIGURE 3. Detailed cost in different cases.

The cost of fuel, grid, maintenance, and environment in each typical working condition is shown in Figure 4. In the three working condition, the fuel cost all accounts for the largest proportion. The fuel cost in winter is the largest compared with other working conditions, when the heat load is very heavy owing to the demand of building heating. The grid

TABLE 5. Detailed cost in different cases ($\times 10^4$ ¥).

Case	Total	C_{inv}	C_{fuel}	C_{grid}	C_{main}	C_{env}
I	3545	268	2,693	10	263	311
II	3540	262	2,723	-21	268	308
III	3414	266	2,571	31	249	298
IV	3212	264	2,335	122	227	265

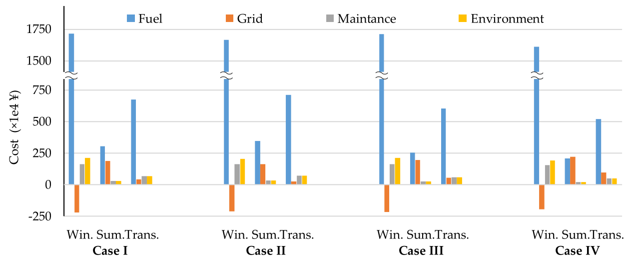

FIGURE 4. The cost of fuel, grid, maintenance, and environment in different typical working condition.

cost is all negative in winter in the four cases owing to selling large amount to the grid. In summer, the heat load is low and the MES buys more electricity from the grid so that the grid cost is positive and considerable, even larger than the fuel cost in the case IV. In transition seasons, the heat load is more than that in summer but less than that in winter and thus, the gas turbine can basically meet the electrical load and the heat load simultaneously and the grid cost is positive but not high.

C. OPERATION ANALYSIS

In order to further reveal the performance of the proposed planning method, the operation condition of the MES in the case IV is analyzed in the following. The electrical power of each devices in the MES in three typical working conditions is shown in Figure 5. In winter, the gas turbine runs all the day to meet the heat load and a large amount of electricity is sold to the grid during 00:00-15:00 and 23:00-24:00. In summer, the output of the gas turbine is very low during 00:00-00:07, 12:00-16:00, and 19:00-14:00 so that most of the electrical demand is meet by the grid. Obviously, in summer when the heat load is very low, the gas turbine has large output only during peak load time. In transition seasons, the gas turbine has high output during 08:00-12:00 and 17:00-21:00 and the MES does not buy electricity from the grid during the peak load time. In summary, the utilization ratio of the gas turbine is high in both winter and transition seasons but low in summer.

The output of the gas boiler in three typical working conditions is shown in Figure 6. It can be seen that the gas boiler does not work in summer and transition seasons because the heat load is very low and can be meet by the gas turbine. In winter, the gas turbine does not work during 00:00-02:00, 08:00-10:00, 15:00-16:00, and 20:00-21:00. During other

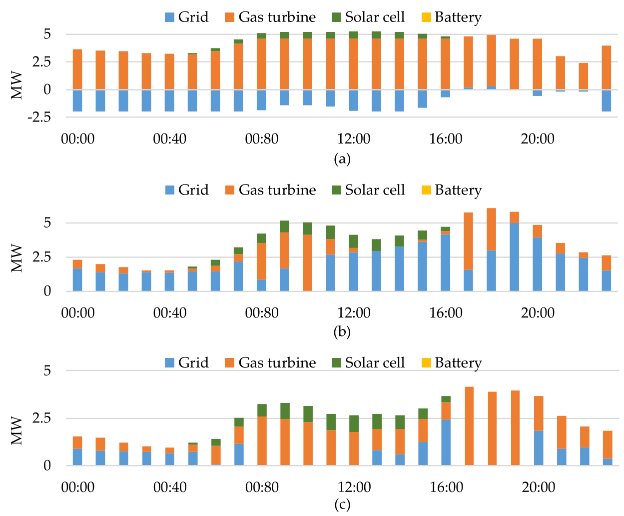

FIGURE 5. Electrical power of each devices: (a) Winter, (b) summer, and (c) transition seasons.

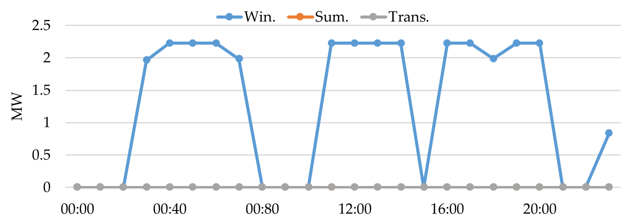

FIGURE 6. Output thermal power of boiler.

time, the output of the gas boiler is very high and nearly at the full load.

IV. CONCLUSIONS

We propose an optimal planning method for the MES that takes into consideration the characteristics of the heating network and the heat load in this paper. The cogeneration system, the heating network, and the heat load including building heating load and domestic hot water load are comprehensibly modeled and embedded into the planning model. Four cases based on the conditions in North China are studied and many interesting conclusions are obtained: (1) considering the characteristics of the heating network and the heat load has no obvious influence on the optimal capacity of the gas turbine but can effectively decrease the necessary capacity of the gas boiler, the battery, and the thermal storage tank; (2) embedding the characteristics of the heating network and the heat load into the planning model has just a little influence on the investment cost, but it brings considerable reduction in the fuel cost; and (3) the gas turbine has a good utilization ratio in winter and transition seasons and in summer it has high output only at peak load time.

REFERENCES

[1] G. Mendes, C. Ioakimidis, and P. Ferrão, "On the planning and analysis of integrated community energy systems: A review and survey of available tools," (in English), *Renew., Sustain. Energy Rev.*, vol. 15, no. 9, pp. 4836–4854, Dec. 2011.

[2] A. P. Prato, F. Strobino, M. Broccardo, and L. P. Giusino, "Integrated management of cogeneration plants and district heating networks," *Appl. Energy*, vol. 97, pp. 590–600, Sep. 2012.

[3] P. Mancarella, "MES (multi-energy systems): An overview of concepts and evaluation models," (in English), *Energy*, vol. 65, pp. 1–17, Feb. 2014.

[4] Y. Zhao, K. Peng, B. Xu, H. Li, Y. Liu, and X. Zhang, "Bilevel optimal dispatch strategy for a multi-energy system of industrial parks by considering integrated demand response," *Energies*, vol. 11, no. 8, p. 1942, 2018, doi: 10.3390/en11081942.

[5] K. Amber, T. Day, N. Ratyal, A. Kiani, and R. Ahmad, "Techno, economic and environmental assessment of a combined heat and power (CHP) system—A case study for a University campus," *Energies*, vol. 11, no. 5, p. 1133, 2018, doi: 10.3390/en11051133.

[6] X. Dong, C. Quan, and T. Jiang, "Optimal planning of integrated energy systems based on coupled CCHP," *Energies*, vol. 11, no. 10, p. 2621, 2018, doi: 10.3390/en11102621.

[7] Y. Wang, Y. Huang, Y. Wang, H. Yu, R. Li, and S. Song, "Energy management for smart multi-energy complementary micro-grid in the presence of demand response," (in English), *Energies*, vol. 11, no. 4, p. 974, Apr. 2018.

[8] S. Rotger-Griful, R. H. Jacobsen, D. Nguyen, and G. Sorensen, "Demand response potential of ventilation systems in residential buildings," (in English), *Energy Buildings*, vol. 121, pp. 1–10, Jun. 2016.

[9] M. Turski and R. Sekret, "Buildings and a district heating network as thermal energy storages in the district heating system," *Energy Buildings*, vol. 179, pp. 49–56, Nov. 2018.

[10] T. Ma, J. Wu, L. Hao, W.-J. Lee, H. Yan, and D. Li, "The optimal structure planning and energy management strategies of smart multi energy systems," *Energy*, vol. 160, pp. 122–141, Oct. 2018.

[11] D. Yu, H. Liu, G. Yan, J. Jiang, and S. Le Blond, "Optimization of hybrid energy storage systems at the building level with combined heat and power generation," (in English), *Energies*, vol. 10, no. 5, p. 606, May 2017.

[12] P. Gabrielli, M. Gazzani, E. Martelli, and M. Mazzotti, "Optimal design of multi-energy systems with seasonal storage," *Appl. Energy*, vol. 219, pp. 408–424, Jun. 2018.

[13] S. Lu, Y. Li, and H. Xia, "Study on the configuration and operation optimization of CCHP coupling multiple energy system," *Energy Convers. Manage.*, vol. 177, pp. 773–791, Dec. 2018.

[14] V. H. Bui, A. Hussain, H. M. Kim, and Y. H. Im, "Optimal energy management of building microgrid networks in islanded mode considering adjustable power and component outages," (in English), *Energies*, vol. 11, no. 9, p. 2351, Sep. 2018.

[15] H. Cai, C. Ziras, S. You, R. Li, K. Honoré, and H. W. Bindner, "Demand side management in urban district heating networks," *Appl. Energy*, vol. 230, pp. 506–518, Nov. 2018.

[16] J. Wang, H. Zhong, Z. Ma, Q. Xia, and C. Kang, "Review and prospect of integrated demand response in the multi-energy system," (in English), *Appl. Energy*, vol. 202, pp. 772–782, Sep. 2017.

[17] N. Kampelis, E. Tsekeri, D. Kolokotsa, K. Kalaitzakis, D. Isidori, and C. Cristalli, "Development of demand response energy management optimization at building and district levels using genetic algorithm and artificial neural network modelling power predictions," *Energies*, vol. 11, no. 11, p. 3012, 2018.

[18] S. Lu, W. Gu, J. Zhou, X. Zhang, and C. Wu, "Coordinated dispatch of multi-energy system with district heating network: Modeling and solution strategy," (in English), *Energy*, vol. 152, pp. 358–370, Jun. 2018.

[19] Z. Li, W. Wu, J. Wang, B. Zhang, and T. Zheng, "Transmission-constrained unit commitment considering combined electricity and district heating networks," (in English), *IEEE Trans. Sustain. Energy*, vol. 7, no. 2, pp. 480–492, Apr. 2016.

[20] A. Shabanpour-Haghighi and A. R. Seifi, "Effects of district heating networks on optimal energy flow of multi-carrier systems," (in English), *Renew., Sustain. Energy Rev.*, vol. 59, pp. 379–387, Jun. 2016.

[21] A. Franco and F. Bellina, "Methods for optimized design and management of CHP systems for district heating networks (DHN)," *Energy Convers. Manage.*, vol. 172, pp. 21–31, Sep. 2018.

[22] F. Brahman, M. Honarmand, and S. Jadid, "Optimal electrical and thermal energy management of a residential energy hub, integrating demand response and energy storage system," (in English), *Energy Buildings*, vol. 90, pp. 65–75, Mar. 2015.

[23] A. Anvari-Moghaddam, A. Rahimi-Kian, M. S. Mirian, and J. M. Guerrero, "A multi-agent based energy management solution for integrated buildings and microgrid system," (in English), *Appl. Energy*, vol. 203, pp. 41–56, Oct. 2017.

[24] M. C. Di Piazza, G. La Tona, M. Luna, and A. Di Piazza, "A two-stage energy management system for smart buildings reducing the impact of demand uncertainty," *Energy Buildings*, vol. 139, pp. 1–9, Mar. 2017.
[25] M. Nistor and C. H. Antunes, "Integrated management of energy resources in residential buildings—A Markovian approach," *IEEE Trans. Smart Grid*, vol. 9, no. 1, pp. 240–251, Jan. 2018.
[26] S. Bahrami and A. Sheikhi, "From demand response in smart grid toward integrated demand response in smart energy hub," (in English), *IEEE Trans. Smart Grid*, vol. 7, no. 2, pp. 650–658, Mar. 2016.
[27] Z. Wang, Y. Tang, X. Chen, X. Men, J. Cao, and H. Wang, "Optimized daily dispatching strategy of building-integrated energy systems considering vehicle to grid technology and room temperature control," (in English), *Energies*, vol. 11, no. 5, p. 1287, May 2018.

HONGZHONG CHENG is currently an Engineer with State Grid Suzhou Power Supply Company. His research interests include renewable energy technology and active distribution networks.

JIAN WU is currently with State Grid Suzhou Power Supply Company, Suzhou, China. His research interests include active distribution networks and power systems operation.

ZHAO LUO received the B.S. degree in electronic science and technology from the Nanjing University of Posts and Telecommunications, China, in 2008, and the M.S. and Ph.D. degrees in electrical engineering from Southeast University, China, in 2013 and 2018, respectively.

He is currently a Lecturer with the Faculty of Electric Power Engineering, Kunming University of Science and Technology. His research interests include distributed generations microgrids and active distribution networks.

FEI ZHOU is currently with State Grid Suzhou Power Supply Company, Suzhou, China. His research interests include active distribution networks and power systems operation.

XINGLIN LIU is currently pursuing the master's degree with the Faculty of Electric Power Engineering, Kunming University of Science and Technology, Kunming, China. Her research interests include distributed generations and microgrids.

TAO LU is currently pursuing the master's degree with the Faculty of Electric Power Engineering, Kunming University of Science and Technology, Kunming, China. Her research interests include distributed generations and microgrids.